

## MIT Open Access Articles

*Tungsten impurity transport experiments in Alcator C-Mod to address high priority research and development for ITER*

The MIT Faculty has made this article openly available. **Please share** how this access benefits you. Your story matters.

**Citation:** Loarte, A. et al. "Tungsten Impurity Transport Experiments in Alcator C-Mod to Address High Priority Research and Development for ITER." *Physics of Plasmas* 22, 5 (May 2015): 056117  
© 2015 AIP Publishing

**As Published:** <http://dx.doi.org/10.1063/1.4921253>

**Publisher:** American Institute of Physics (AIP)

**Persistent URL:** <http://hdl.handle.net/1721.1/111188>

**Version:** Author's final manuscript: final author's manuscript post peer review, without publisher's formatting or copy editing

**Terms of Use:** Article is made available in accordance with the publisher's policy and may be subject to US copyright law. Please refer to the publisher's site for terms of use.



PSFC/JA-14-34

## **Tungsten Impurity Transport Experiments in Alcator C-Mod to Address High Priority R&D for ITER**

Loarte<sup>1</sup>, A., Reinke<sup>2</sup>, M.L., Polevoi<sup>1</sup>, A.R., Chilenski, M.,  
Howard, N.T., Hubbard, A., Hughes, J.W., Rice, J.E., Walk, J.,  
Kochl<sup>3</sup>, F., Putterich<sup>4</sup>, T., Dux<sup>4</sup>, R. and Zhogolev<sup>5</sup>, V.E.

<sup>1</sup>ITER Organization, St. Paul Lez Durance, Cedex, France

<sup>2</sup>University of York, York, UK

<sup>3</sup>Technische Universität Wien, Vienna, Austria

<sup>4</sup>Max-Planck-Institut für Plasmaphysik, Garching, Germany

<sup>5</sup>Kurchatov Institute, Moscow, Russia

December, 2014

**Plasma Science and Fusion Center  
Massachusetts Institute of Technology  
Cambridge MA 02139 USA**

This work was supported in part by the U.S. Department of Energy, Grant No.DE-FC02-99ER54512. Reproduction, translation, publication, use and disposal, in whole or in part, by or for the United States government is permitted.

# **Tungsten impurity transport experiments in Alcator C-Mod to address high priority R&D for ITER**

A. Loarte

ITER Organization, Route de Vinon-sur-Verdon, CS 90 046, 13067 St Paul Lez Durance  
Cedex, France

M.L. Reinke

York Plasma Institute, Department of Physics, University of York, Heslington. York, YO10  
5DD, United Kingdom

A.R. Polevoi

ITER Organization, Route de Vinon-sur-Verdon, CS 90 046, 13067 St Paul Lez Durance  
Cedex, France

M. Chilenski, N. Howard, A. Hubbard, J.W. Hughes, J.E. Rice, J. Walk and the Alcator C-  
Mod Team

Plasma Science and Fusion Center, Massachusetts Institute of Technology, Cambridge,  
Massachusetts 02139, USA.

F. Köchl

Technische Universität Wien, Atominstitut, Stadionallee 2, 1020 Vienna, Austria

T. Pütterich, R. Dux

Max-Planck-Institut für Plasmaphysik, Boltzmanstraße 2, D-85748 Garching, Germany

V. E. Zhogolev

NRC "Kurchatov Institute", Kurchatov square 1, 123098 Moscow, Russia

**Abstract.** Experiments in Alcator C-Mod tokamak plasmas in the Enhanced D-alpha (EDA) H-mode regime with ITER-like mid-radius plasma density peaking and Ion Cyclotron Resonant heating (ICRH), in which tungsten is introduced by the laser blow-off technique, have demonstrated that accumulation of tungsten in the central region of the plasma does not take place in these conditions. The measurements obtained are consistent with anomalous transport dominating tungsten transport except in the central region of the plasma where tungsten transport is neoclassical, as previously observed in other devices with dominant neutral beam injection heating such as JET and ASDEX Upgrade. In contrast to such results, however, the measured scale lengths for plasma temperature and density in the central region of these Alcator C-Mod plasmas, with density profiles relatively flat in the core region due to the lack of core fuelling, are favourable to prevent inter and intra sawtooth tungsten

accumulation in this region under dominance of neoclassical transport. Simulations of ITER H-mode plasmas including both anomalous (modelled by the Gyro-Landau-Fluid code GLF23) and neoclassical transport for main ions and tungsten and with density profiles of similar peaking to those obtained in Alcator C-Mod show that accumulation of tungsten in the central plasma region is also unlikely to occur in stationary ITER H-mode plasmas due to the low fuelling source by the neutral beam injection (injection energy  $\sim 1\text{MeV}$ ), which is in good agreement with findings in the Alcator C-Mod experiments.

## 1. Introduction.

The next generation of fusion devices, such as ITER, is expected to operate with tungsten (W) plasma facing components (PFCs) and in regimes with high energy confinement in order to demonstrate high fusion power amplification [Campbell 2012]. Due to its high electronic charge, W remains partially ionized in the plasma, even for the range of temperatures expected in the central region of the plasma in ITER ( $T_e \sim 10\text{-}30$  keV), thus causing large radiative power losses from the plasma by line emission of the partially ionized W atoms excited by electron impact. As a consequence, the concentrations of W in the confined plasmas which are compatible with high energy confinement and high fusion power amplification in nuclear fusion reactors are very low (typically few  $10^{-5}$ ) [Kallenbach 2005]. The need to control the concentration of W in the confined plasma is not restricted to next step fusion devices but it is already required for present tokamak experiments. Lack of W concentration control causes the radiated losses from the plasma to approach or exceed the plasma heating power, which triggers MHD instabilities that usually end up in a disruption [de Vries 2012].

Operation in the H-mode high energy confinement regime is more challenging from the W concentration control point of view due to the formation of a region with very low anomalous transport at the plasma edge (edge transport barrier or ETB). In the ETB impurity transport is found to be well described by neoclassical transport for low-Z to mid-Z impurities [Pütterich 2011] which, for typical edge density and temperature profiles in present experiments, has an inward convective velocity component [Sunn Pedersen 2000]. This leads to peaked W profiles in the ETB region with values of the W concentration in the inner part of the ETB much larger than those near the plasma separatrix. Production of W by sputtering of the PFCs together with the unfavourable transport in the ETB can lead to the uncontrolled increase of the W concentration in the edge of the confined plasma in the absence of other processes. This edge W concentration increase is arrested by the occurrence of edge MHD instabilities (ELMs) which cause an expulsion of particles from the edge plasma or by enhanced edge turbulence observed in H-mode regimes which either do not have ELMs such as the EDA (Enhanced D-alpha) H-mode confinement regime [Greenwald 1999] or in which 3-D magnetic field perturbations are applied to suppress them [Evans 2006]. Control of ELMs and of the divertor W erosion source between the ELMs is expected to be appropriate to provide the required level of W concentration control in the region of the ETB in ITER [Loarte 2014].

The control of the W concentration to an acceptable level in the edge plasma region in H-modes is a necessary but not sufficient condition to ensure that the concentration of W in the central region of the plasma remains low enough to prevent excessive radiation, which leads to the termination of the high confinement H-mode regime. Uncontrolled increases of the core W concentration (for quasi-stationary values of the edge W concentration) are frequently observed for H-mode discharges in tokamaks operating with W PFCs whose plasma heating is dominated by neutral beam injection (NBI) [Neu 2002]. The physics picture recently demonstrated to explain this phenomenology in H-mode plasmas is that W transport is dominated by anomalous transport for most of the plasma cross section inside the ETB except the very central region close to the magnetic axis [Pütterich 2013, Angioni 2014a, Casson 2014]. In this central region W anomalous transport is negligible and W transport is dominated by neoclassical effects, similar to earlier ASDEX Upgrade observations using extrinsic seeding of noble gases [Dux 1999]. Therefore, peaking of the W density in the central plasma region is determined by the competition between the ion density radial gradient (which produces an inward W flux) and the ion temperature radial gradient (which produces an outwards W flux usually called temperature screening). In experiments with dominant NBI heating the ion density and temperature gradients are often such that their net effect is to drive a significant inward flow leading to strong peaking of the W density profile [Angioni 2014a]. An important factor in this behaviour is the fact that NBI heating unavoidably provides a source of neutrals in the central plasma region thus leading to a sizeable peaking of the ion density profile there [Mantica 2014]. This relation between the ion density and temperature gradients in the central region of the plasma for NBI dominated plasmas can be modified by the application of central RF heating (ECRH and ICRH) thus avoiding an uncontrolled increase of the core W density [Neu 2002, Goniche 2014]. This picture is complicated by the role that these additional heating systems play in sustaining poloidal variations in high-Z impurity density, which is shown to have an important impact on the flux-surface averaged neoclassical radial impurity transport [Angioni 2014b]. Sustained MHD activity [Angioni 2014a, Pütterich 2013] may also complicate this picture, but experiments and simulations discussed here focus plasmas that are MHD-free or have resolvable, discrete MHD events (i.e. sawteeth).

Despite the wide range of experimental results regarding W density peaking in the central plasma described above, their implications for ITER remain uncertain. This is due to differences between ITER and present experiments beyond those associated with the larger

device size and plasma parameters (which may lead to different physics processes dominating plasma turbulent transport), such as:

a) heating schemes, which are dominated by electron heating in ITER versus present experiments most of which are ion heating dominated.

b) central plasma fuelling, whose rate is typically one order of magnitude or more smaller in ITER than in present experiments due to the high energy of the NBI injected particles ( $\sim 1$  MeV in ITER versus 50-100 keV in present experiments). When the plasma volume is taken into account, the fuelling rate per unit volume in the central plasma of ITER is typically two to three orders of magnitude smaller than in present experiments

c) plasma toroidal rotation which is expected to have a low Mach number in ITER (in the absence of large intrinsic rotation) due to the lower momentum input by the NBI due to their higher injection energy and which is known to affect  $W$  neoclassical transport [Angioni 2014a, Casson 2014].

All these factors together with differences in the underlying shape of the plasma density and temperature profiles between present experiments and ITER, which influence  $W$  transport, make impossible a straightforward extrapolation of the present experimental results to ITER.

This paper describes the results of modelling studies of  $W$  transport for ITER reference operational conditions and the results of a series of experiments on the Alcator C-Mod tokamak to characterize  $W$  transport in conditions similar to those expected in ITER in terms of: a) core electron density and ion and electron temperature peaking, b) plasma toroidal rotation, c) dominant electron heating and d) low/no source of neutrals injected by the heating systems in the plasma central region.

The paper is organised as follows: section 2 summarizes the results of the modelling studies of  $W$  transport for the reference 15MA/5.3T high fusion gain  $Q_{DT} = 10$  scenario in ITER, section 3 describes plasma conditions and experimental techniques utilized to characterize  $W$  transport in the Alcator C-Mod experiments, section 4 describes the results concerning  $W$  transport in Alcator C-Mod and its dependencies on discharge parameters and finally section 5 summarises the results in view of their extrapolation to ITER, draws conclusions and discusses future directions for Alcator C-Mod R&D in this area.

## **2. Modelling of $W$ transport in ITER.**

Modelling of  $W$  transport for the ITER core plasma has been carried out with the ASTRA modelling code, which includes a model for anomalous main ion and  $W$  transport based on the GLF23 transport model [Pereverzev 2002, Waltz 1997]. In addition to anomalous transport, neoclassical transport is evaluated with transport coefficients obtained

from the NCLASS code [Houlberg 1997] for main ions and W impurities. Impurity transport is modelled by the code ZIMPUR [Leonov 2005] which is coupled to the main plasma ion transport in ASTRA. In all the simulations performed for ITER the value of the W density at the plasma edge is set as a boundary conditions with low concentration values ( $< 10^{-5}$ ) so that the W radiative losses from the main plasma are low and do not affect the core plasma parameters. This is appropriate for the purpose of these studies as they focus on the determination of whether the W density profile will be strongly peaked with respect to the main ion density profile in ITER or not. The evaluation of the expected W level in ITER requires more sophisticated modelling including the effect of controlled ELMs on W expulsion and production of W by sputtering from the divertor and its transport in the scrape-off layer (SOL), which is beyond the scope of this paper. The modelling assumptions are thus:

- Plasma conditions in the ETB region are evaluated by predictions of the EPED model [Snyder 2011] and used as boundary conditions for the studies of core plasma transport
- Energy and particle transport for main ions and W is provided by the sum of the contributions from anomalous transport (evaluated with the GLF23 model) and neoclassical transport evaluated with NCLASS so that:

$$\begin{aligned}
 \blacksquare \quad \chi_{e,i} &= \chi_{i\text{-neo}} + \chi_{e,i\text{-GLF}} \\
 \blacksquare \quad D_{i,W} &= D_{i,W\text{-neo}} + D_{i,W\text{-GLF}} \\
 \blacksquare \quad V_{i,W} &= V_{i,W\text{-neo}} + V_{i,W\text{-GLF}} \\
 \blacksquare \quad \chi_{\text{momentum}} &= \chi_{i\text{-neo}} + \text{Pr} \times \chi_{i\text{-GLF}}
 \end{aligned}$$

where subscripts with the neo suffix refers to the values evaluated on the basis of neoclassical transport and the GLF suffix refers to those from anomalous transport,  $\chi_e$  and  $\chi_i$  are the heat diffusivities for electrons and main ions respectively,  $D_{i,W}$  and  $V_{i,W}$  are the particle diffusivities and particle velocity pinches for the main ions and W respectively, and  $\chi_{\text{momentum}}$  is the momentum diffusivity for the main ions and Pr is the Prandtl number. For the electrons the value of heat diffusivity when anomalous transport is negligible is set to that of ion neoclassical transport; otherwise the very low value of the electron neoclassical thermal diffusivity ( $\chi_{e\text{-neo}} \sim 1/60 \times \chi_{i\text{-neo}}$ ) leads to unphysical high electron temperatures in the simulations. This reflects the fact that reduction of electron and ion turbulent heat transport under the level of ion neoclassical heat transport predictions is not commonly observed in experiments (for instance, in the ETB electron and ion heat transport are commonly observed



to reduce to levels of ion neoclassical heat transport, which is a factor of  $\sim 60$  higher than electron neoclassical heat transport).

ITER simulations have been carried out for the ITER DT plasmas in stationary phases of the reference high fusion gain scenario ( $Q_{DT}=10$ ) with plasma current of 15 MA and toroidal field of 5.3 T and for a lower current/toroidal field plasma (7.5 MA/2.65 T), representing typical low current plasmas in which initial H-mode operation will be developed in DT in ITER. For both cases additional heating power of  $\sim 50$ -53 MW has been applied with 33 MW of NBI heating and the remaining 17-20 MW from radiofrequency heating (ICRH or ECRH). It should be noted that in the ITER reference high  $Q_{DT}$  scenario the dominant plasma heating ( $\sim 100$  MW) is provided by alpha particles produced by the fusion reactions which thermalize in the plasma. The results regarding plasma W transport in both ITER scenarios are qualitatively similar; thus we only will describe in detail the studies for the 15 MA/5.3 T plasma as this is more relevant regarding the achievement of ITER mission's and for fusion tokamak reactors in general.

The plasma parameters obtained for a range of simulations for the ITER 15 MA/5.3 T  $Q_{DT} \sim 10$  plasma applying different heating schemes (33 MA of NBI + 20 MW of off axis or on axis ECRH and 33 MA of NBI + 20 MW of on axis ICRH with  $\text{He}^3$  minority to provide maximum ion heating) are shown in Fig. 1 a-d. As previously identified, for the typical conditions expected in ITER the plasma density profile is moderately peaked  $n_i(0)/n_{i-ped} \sim 1.6$  despite the low level of core NBI fuelling. This is due to the existence of an anomalous inward plasma pinch over most of the cross section of the ITER plasma [Angioni 2007] which is correctly predicted by the GLF23 model. It should be noted that in these simulations the Prandtl number has been adjusted (to the same value for all simulations) so that the plasma thermal energy agrees with expectations from the ITER-98 energy confinement time scaling law (i.e.  $H_{98} = 1$ ) [IPB 1999] leading to a fusion performance of  $Q_{DT} \sim 10$  for the expected values of the pedestal pressure in the ETB predicted by the EPED model [Snyder 2011]. The value of the Prandtl number affects toroidal rotation shear which in turn affects the stiffness of the ion temperature profile predicted by the GLF23 model and the predicted fusion performance. It is well known that, without inclusion of rotational shear effects weakening the ion temperature stiffness and with a pedestal pressure value in agreement with the EPED model, the anomalous transport from the GLF23 model predicts a fusion performance for ITER 15 MA/5.3T plasmas of  $Q_{DT} \sim 6$ -7 [Parail 2013].

The predicted W density profiles and anomalous W transport for these three ITER simulations are shown in Fig. 2.a-b. As can be seen in Fig.2.a the W density profiles are flat

over most of the plasma cross section and in the central part they can be somewhat peaked but with similar  $n_W(0)/n_{W-ped}$  to  $n_i(0)/n_{i-ped}$  or lower and thus similar W concentration across the plasma cross section. Of the three cases considered, the one with the highest W peaking is that with off-axis ECRH heating. The physics processes that lead to this W density profile shapes can be understood from Fig.2.b. For these plasma conditions W transport is found to be dominated by anomalous transport over most of the plasma cross section ( $r > 0.25-0.4$  m) with a large diffusion coefficient (shown in Fig. 2.b) and very low anomalous pinch (not shown). In the very central part of the plasma ( $r < 0.25-0.4$  m) anomalous transport is negligible and neoclassical W transport dominates. Thus whether W is more or less peaked in this region depends on the relative scale lengths of the ion density and temperature profiles in this region. Application of central heating (whether pure electron heating with ECRH or mixed ion-electron heating with He<sup>3</sup> minority ICRH heating) changes the relative scales of the ion density and temperature profile in this region and correspondingly decreases the central values of the W density (see Fig. 3), as the intensity of temperature screening increases with respect to the inward flux driven by the ion density gradient. It should be noted that in the simulations the effect of central electron heating and ion heating are different although they produce a similar result regarding W transport. Central electron heating increases the ion density scale length (at  $\sim$  constant ion temperature scale length) while ion heating decreases the ion temperature scale length (at  $\sim$  constant electron and ion density scale lengths). This is somewhat different from results on ASDEX-U which showed ECRH and ICRH both reducing the W peaking, but the former through increasing W anomalous diffusion and the later through reduced inward neoclassical convection [Dux 2003].

The effectiveness of central RF heating ( $P_{RF} = 20$  MW) to affect the main ion temperature and density profiles despite the dominance of alpha heating ( $P_\alpha = 100$  MW) can be understood because of the much more peaked power deposition profiles of the heating provided by RF than by alpha heating. Table 1 shows the calculated power densities in electron and ions for the two cases for ITER plasmas with 15 MA/5.3T –  $Q_{DT} = 10$  with central RF heating described above. From the values in this table it is clear that the ITER RF heating systems have the capabilities to increase the power density in the central region which is deposited in the electrons by a factor of 2-3 above that of the value from alpha heating and for the ions by up to a factor of 2, despite the integral heating power from alpha heating being five times higher than that of the RF one. If the temperatures profiles are non-stiff in the core region this will lead to a decrease of the temperature scale length (improved temperature screening seen for central ICRH heating in Fig. 3). If, on the contrary, the temperature

profiles are very stiff in this central region this will lead to no change in the temperature profile but to an increase of anomalous transport that flattens the density profile (reduced inward W transport seen for central ECRH heating in Fig. 3).

The results of these modelling studies for ITER are in excellent qualitative agreement with recent studies of W transport and W peaking in JET experiments [Angioni 2014a, Casson 2014] and its control by ICRH heating (electron heating) [Goniche 2014]. These studies also find that large diffusive anomalous W transport dominates inside the ETB except for the very central region of the plasma where W transport is neoclassical. In agreement with these studies the ITER simulations only find indications of central peaking in the W density profile when

$$\frac{a}{Ln_i} - \frac{a}{2L_{T_i}} > 0 \quad (1)$$

i.e. for the case with off-axis ECRH heating. Despite this, there are significant quantitative differences between the predicted W transport in ITER and in these JET experiments. Some of them are linked to the low values of plasma rotation in these ITER simulations ( $M_{DT} \leq 0.1$ ) compared to those of JET ( $M_{DT} \sim 0.4$ ) [Angioni 2014a], which can strongly increase the magnitude of the neoclassical transport coefficients for W due to centrifugal effects. Others are linked to the magnitude of the central source provided in ITER by the neutral beam injection compared to the ion heating power density and to its implications for the ratio of the ion density and temperature scale lengths in the core plasma region, which is given by:

$$\frac{Ln_i}{L_{T_i}} = \frac{D_i q_i}{\chi_i \Gamma_i T_i} \quad (2)$$

Taking into account the central plasma conditions in the ITER  $Q_{DT}=10$  plasmas ( $q_i \sim 0.35 \text{ MWm}^{-3}$ ,  $\Gamma_i \sim 3 \cdot 10^{17} \text{ m}^{-3}\text{s}^{-1}$ ,  $T_i \sim 20 \text{ keV}$ ) and those of the JET plasmas in [Angioni 2014a] plasmas ( $q_i \sim 0.6 \text{ MWm}^{-3}$ ,  $\Gamma_i \sim 7 \cdot 10^{19} \text{ m}^{-3}\text{s}^{-1}$ ,  $T_i \sim 5 \text{ keV}$ ) and assuming that in the central plasma region  $D_i/\chi_i$  is independent of device size (this is the case for neoclassical transport)

leads to:

$$\frac{\left. \frac{Ln_i}{L_{T_i}} \right|_{JET}}{\left. \frac{Ln_i}{L_{T_i}} \right|_{ITER}} = \frac{q_i^{JET} \Gamma_i^{ITER} T_i^{ITER}}{q_i^{ITER} \Gamma_i^{JET} T_i^{JET}} \sim 0.03 \quad (3)$$

showing a clear trend for the ion density profiles to be much more peaked relative to the ion temperature profiles in the JET experiments in [Angioni 2014a] than those for typical ITER  $Q_{DT} = 10$ . The JET and ASDEX Upgrade NBI-dominated experiments are thus in a situation more prone to core W accumulation than ITER  $Q_{DT} = 10$  plasmas.

While these modelling results and considerations for ITER are very encouraging for the situation concerning W transport in the core plasma of ITER, significant uncertainties remain regarding the modelling results, such as:

- a) the accuracy with which any model for anomalous transport can predict the gradients for density and temperature in the region where anomalous transport is dominant.
- b) the extent of the region in the plasma centre in which anomalous transport is low.
- c) the level of residual electron transport in this central region.
- d) the role of sawteeth in affecting W transport. Although initial ITER simulations including the effect of sawteeth do not show a different qualitative picture that when they are not included for ITER, the model for W expulsion by sawteeth as well as the recovery of the plasma density and temperature following the sawteeth are subject to modelling uncertainties due to the large gradients that can be transiently formed.

Therefore, it is required to validate if the positive trends regarding W transport in the core plasma identified in the ITER modelling are indeed found in the experiment. For this purpose a series of experiments was carried out in the Alcator C-Mod tokamak to characterize W transport in conditions that match specific aspects of the ITER plasmas which have been found by modelling to have significant effects on W transport in the core plasma.

### **3. Overview of experiments in Alcator C-Mod.**

Alcator C-Mod [Hutchinson 1994, Marmar 2007] is a compact, high field tokamak with vertical plate divertor geometry and RF-based heating and current-drive systems (LHCD and ICRH). The experiments reported in this paper were carried out with central ICRH heating of plasmas in the EDA H-mode confinement regime [Greenwald 1999]. The EDA H-mode is an ELM-less H-mode plasma in which density transport is enhanced by the presence of a quasi-coherent mode at the plasma edge which arrests the density rise typical of ELM-free H-mode and prevents the uncontrolled increase of impurities in the core that would otherwise lead to excessive bulk plasma radiation even in the absence of a large core impurity peaking [Rice 1997, Rice 2000, Sunn Pedersen 2000, Rice 2007]. Steady high performance EDA H-modes have similar pedestal pressure profiles to those obtained in ELM-free H-

modes [Hughes 2007], and only a slight reduction in maximum normalised energy confinement results from the EDA onset [Greenwald 1999].

The quasi-coherent mode also prevents the plasma from reaching unstable edge pressure/current gradients and thus triggering edge instabilities known as ELMs. Because of the large erosion of ITER PFCs [Federici 2003] and the detrimental effects on plasma performance of impurity influxes produced by ELMs, the maximum loss of energy during ELMs must be significantly reduced in ITER from its expected “natural” or “uncontrolled” values by large factors (typically  $\sim 30$  for  $Q_{DT}=10$  plasmas) by controlled triggering of ELMs [Loarte 2014]. Controlled ELMs are also required to provide appropriate W exhaust from the confined plasma in ITER even for conditions in which uncontrolled ELMs would be acceptable from the divertor erosion point of view [Loarte 2014]. In this respect, the EDA regime in Alcator C-Mod represents a good proxy for the controlled ELM regimes required in ITER.

The experiments described in this paper were carried out with a plasma current of 0.44-0.6 MA and a toroidal field of 5.4 T, corresponding to  $q_{95} = 6 - 8$ , with the ion grad-B direction favourable for H-mode access in a lower single null diverted plasma configuration. All discharges were heated by ICRH and the ICRH heating power into the plasma spanned the range from 1.0 – 3.6 MW. The lower limit was dictated by access to the H-mode regime while the upper limit was defined either by the maximum ICRH power that could be reliably coupled to the plasma (for 0.6 MA) or by acceptable loads at the limiters from ions accelerated by the ICRH (for plasma currents of 0.44 and 0.52 MA). The plasma line average density normalized to the Greenwald limit was typically  $\langle n_e \rangle / n_{GW} \sim 0.3-0.4$  in these experiments and the effective plasma collisionality was  $1.0 < \nu_{EFF} < 4.0$  [Angioni 2007]. These relatively low current/high  $q_{95}$  (much larger than for  $Q_{DT} = 10$  operation in ITER) and high ICRH heating power plasmas were chosen to perform these experiments on W transport characterization in Alcator C-Mod because the density peaking obtained in them is similar to that expected in ITER for H-mode operation [Greenwald 2007] and because density peaking is a key factor driving core W accumulation in present experiments and ITER. Other important features of these experiments regarding their possible effect on W transport which are similar to ITER are:

- Dominant electron heating (typically  $q_e/q_i \sim 2-3$ ) provided by the ICRH H-minority heating scheme, similar to typical ratios in ITER;

- Lack of central source of neutral particles, as additional heating is RF-based without neutral beam injection, similar to the situation with 1 MeV beams in ITER;
- Low toroidal rotation (typically  $M_D \leq 0.05$  in these experiments, which is in the low range of toroidal rotation speeds in Alcator C-Mod) similar to that expected in ITER because of the low momentum input with the high energy beams, leading to poloidally symmetric high-Z impurity density.

Experiments were performed by injecting W by the laser blow-off technique (LBO) [Howard 2011]. The key measurements of kinetic plasma parameters used for the studies presented in this paper are: Thomson scattering for the electron density and temperature, electron cyclotron emission for the electron temperature [Basse 2007], X-ray imaging crystal spectrometry for ion temperature and toroidal rotation profile measurements [Reinke 2012]. For the characterization of W transport and plasma radiation evolution associated with the W LBO injection the key measurements are provided by: radially and vertically viewing Soft X-ray tomography by two 38-channel arrays [Basse 2007] (equipped with a 50  $\mu\text{m}$  Be filter), a horizontally viewing midplane AXUV (Absolute eXtreme Ultra-Violet) diode array and set of resistive bolometers [Reinke 2008] and a pair of radially viewing, flat-field VUV spectrometers (1-7 nm, 10-30 nm) [Reinke 2010].

An example of the typical evolution of the plasma parameters in these experiments is shown in Fig. 4 for two ICRH heating power levels. Although the intensity of the laser for W LBO was adjusted to keep the W injection to the minimum required for diagnostic purposes, the associated radiation increase and changes to the edge plasma following the W LBO were sufficient to trigger a back transition into L-mode in the low power (black in Fig. 4) case. This limited the lower range of ICRH power for which W transport could be characterized in H-mode by this technique for some of the conditions explored. At higher powers, as shown in Fig. 4, the effect of the W LBO was much less perturbing and the plasma remained in H-mode without major modifications of its parameters. The electron and ion temperature and electron density from the diagnostics above for the two example discharges in Fig.4 are shown in Fig. 5. As can be seen in Fig. 5 and quantified in Table 2, the overall peaking of the core density and temperature profiles, characterized by the ratio of its values at normalized radius ( $\rho = r/a$ )  $\rho = 0$  and 0.7 are similar for ITER  $Q_{DT}=10$  plasmas and for Alcator C-Mod. If anything, the Alcator C-Mod profiles for high  $P_{ICRH}$  levels are less favourable for W transport (more likely core W peaking) than those of ITER. This is due to the lower level of equipartition in Alcator C-Mod at these densities and to the dominant electron heating which

leads to a large increase of the  $T_e/T_i$  ratio (from 1.4-1.8) as the ICRH power is increased. This is unlike ITER where equipartition is dominant and  $T_e/T_i \sim 1$  despite the dominant electron heating. In general the relation between the ion temperature gradient and the density gradient is found to be favourable for W transport in the central region of the plasma ( $\rho \leq 0.35$ ) if W were dominated by neoclassical transport in this region; while further out the situation is opposite, as shown in Fig. 6. Increasing the central ICRH heating power reduces the scale length of the ion temperature with respect to the density (thus making W neoclassical transport to be outwards in the central region) while further out the effect is opposite.

Regarding other impurity-related transport aspects, these discharges are indeed very comparable to ITER. The toroidal rotation velocity in the core plasma is typically low with  $M_D \leq 0.1$  and, correspondingly, poloidally symmetric impurity profiles are measured for these discharges.

#### **4. Observations on W dynamics and transport in ITER-like H-mode plasmas in Alcator C-Mod.**

An example of the typical evolution of the AXUV and spectroscopic line emission following the W LBO in these experiments is shown in Fig. 7. As shown in this figure the propagation of the radiation increase associated with the propagation of W into the plasma in these experiments is very fast up to  $\rho \sim 0.3$  (within 3 ms); from there inwards transport is much slower and the rise of the W associated emission takes place in timescales of 15 ms. This is confirmed by a similar prompt rise of W unresolved transition array (UTA) emission characteristic of  $W^{27+-35+}$  and a much slower evolution of line emission from  $W^{42+-44+}$ . This temporal evolution of the W emission in the plasma within  $\rho \leq 0.8$  for can be modelled with the STRAHL code [Dux 2006] by assuming a radially variable diffusion coefficient for W transport (without any convective velocity) with a very low value within the  $\rho \leq 0.3$  region ( $D_W \sim 4 \cdot 10^{-2} \text{ m}^2\text{s}^{-1}$ , which is similar to the expected value of the W neoclassical diffusion coefficient in this region). For  $\rho > 0.3$  the value of  $D_W$  required to model the fast propagation of W is typically one to two orders of magnitude larger. These findings are in excellent agreement with expectations for ITER shown in Fig. 2.b.

In agreement with the ITER expectations and with the relation of the density and temperature scale lengths measured in these Alcator C-Mod plasmas (see Fig. 6.a), there is no evidence for strong, steady-state W peaking in the central region of the plasmas in these discharges, as shown in Fig. 8. In this figure the W density profile after penetration of the W injected by LBO to the plasma core is derived from the radiated power profiles from resistive

bolometers and from soft X-ray tomography, averaging over multiple sawteeth. For both ways to evaluate the W profile, this is found to be rather flat in the plasma core and in all cases less peaked than the corresponding electron density profile in the same region. It is important to remark that there is no sign of W density peaking in the outer regions of the plasma ( $0.35 \leq \rho \leq 0.55$ ) even for conditions in which neoclassical transport would predict it on the basis of the local plasma density and ion temperature scale lengths in Fig. 6.a. This is consistent with the fact that in that region W anomalous transport is dominant and that  $D_{W}^{\text{anomalous}} \sim (10-100) D_{W}^{\text{neo}}$  so that the resulting W peaking is one to two orders of magnitude lower than evaluations made on the basis of neoclassical transport alone. Therefore, the peaking of the main ion density caused by anomalous transport in these plasmas (and expected in ITER, which could increase its fusion performance for given edge MHD pressure limits) for  $0.3 < \rho < 0.8$  does not bring associated with it any drawback regarding W density peaking in this region, consistent with the ITER modelling results in Fig.1.a and 2.a.

An interesting issue that has been possible to address in the Alcator C-Mod experiments, and which is difficult to address by modelling for ITER (as discussed in Sect. 2), is whether there is a significant W density peaking between sawteeth in these plasmas with ITER-like sawtooth-averaged peaked plasma density profiles. This has been assessed by analysing the increase of the soft X-ray emission between sawteeth compared to that expected from the change of radiation emission efficiency,  $L_{W,SXR}(T_e)$ , caused by the change of the electron temperature inside the sawtooth inversion radius between sawteeth. As shown in Fig. 9, the increased soft X-ray emissivity due to tungsten:

$$\delta \varepsilon_{SXR} = n_e n_W L_{W,SXR}(T_e) \quad (4)$$

in the plasma central region inside the sawtooth inversion radius can increase by a factor of  $\sim 1.8$  when the electron temperature increases by  $\sim 33\%$  from 3 to 4 keV. This increased peaking of the soft X-ray emission between sawteeth could in principle be due to an increase of the W density itself (i.e. there would be W accumulation between sawteeth and W expulsion from the core by sawteeth) or due to the increased peaking of the temperature. Analysis of the change to the W soft X-ray radiation due to the change of temperature has been carried out by using two sets of W emission modelling for  $L_{W,SXR}$ , following the procedures in [Angioni 2014a] but accounting for the thinner Be filter. This reveals that most of the experimentally observed increase between sawteeth can be attributed to an increase by a factor of 1.4-1.5 of the soft X-ray radiation efficiency when the temperature increases from



3 to 4 keV. The residual increase up to the measured 1.8 could be compatible with an increase of the electron density by  $\sim 10\%$  between sawteeth at constant W concentration.

In order to confirm in detail the conclusions extracted from the sawtooth-averaged W density profile in Fig. 8 and of its possible change between sawteeth in Fig. 9, detailed analysis of the radial scale length of the soft X-ray emission in the core region ( $\rho = 0.15$ ) has been carried out in order to determine what the W density scale length compatible with these measurements is and what could be its variation along the sawtooth cycle. Expanding Eq. 4:

$$\frac{a}{L_\varepsilon} = \frac{a}{L_{n_e}} + \frac{a}{L_{n_W}} + \frac{T_e}{L_W} \frac{dL_W}{dT_e} \frac{a}{L_{T_e}} \quad (5)$$

shows that the emissivity scale length,  $L_\varepsilon$ , can be used as a proxy for the tungsten density scale length,  $L_{n_W}$ . From the experimental data for the measured electron density and temperature scale lengths (see e.g. Fig. 6.b), their variations between sawteeth ( $a/L_{n_e}$  nearly constant and  $a/L_{T_e}$  increasing from 0 to its stiff, sawtooth-averaged value), the deduced values for  $a/L_\varepsilon$  assuming that  $a/L_{n_W} = 0$  are shown in Table 3.

Calculation of the inverse scale length of the soft X-ray emission at  $\rho = 0.15$  shown in Figure 9 indicates little variation between sawteeth (after the initial phase immediately after the flattening of the temperature by the sawtooth) and that a quasi-stationary level is reached during each sawtooth prior to the destabilization of the  $m/n=1/1$  precursor mode. Fig. 10.a shows the trajectories of  $a/L_\varepsilon$  versus  $T_e$  within the sawtooth cycle for an ICRF power scan demonstrating that within the experimental variations of the electron density and temperature scale lengths and of the normalized radiation efficiency with temperature, there is no need to invoke strong W density peaking (i.e. a large  $a/L_{n_W}$  in Eq. 5) to explain the variation of  $a/L_\varepsilon$  in the sawtooth cycle. The range of the inverse scale lengths of the soft X-ray radiation emission in Fig. 10.a is similar to that from expectations in Table 3, which are evaluated on the basis of the assumption of flat W profiles with  $a/L_{n_W} = 0$ . From the upper values of the inverse scale lengths of the soft X-ray radiation emission in Fig. 10.a, a value of  $a/L_{n_W} \sim 1-2$  could be compatible with these experimental measurements. It should be noted that this value of the W density scale length is in good agreement with that from neoclassical transport of W in Alcator C-Mod evaluated with the measured plasma density and ion temperature profiles; i.e.  $a/L_{n_{W\text{neo}}} = aV_W^{\text{neo}}/D_W^{\text{neo}} = 1 - 2$ .

Deviations from this picture have been identified in cases where there is off-normal MHD activity (not discussed in this paper) and when the H minority density has been increased from the usual the 3-4% to a much higher level of 10%. This is shown in Figure 10.b, where strong peaking of the soft X-ray radiation emission is found between sawteeth

which is well above the range of values in Table 3 and indicate that strong W peaking takes place in these conditions. When the hydrogen level is increased by main-chamber H<sub>2</sub> puffing at fixed power,  $a/L\epsilon$  increases by a factor of 3, while increasing the ICRF power at  $H/(H+D) \sim 0.1$  reduces the emissivity peaking. This is believed to be due to the influence of friction between the high energy minority ions and the W ions, which is well described by neoclassical transport along the initial modelling studies in [Casson 2014]. This will be the subject of further modelling and experimental studies in Alcator C-Mod.

## 5. Summary, Conclusions and further R&D.

The results obtained in the Alcator C-Mod experiments described in this paper have provided for the first time an experimental characterization of the behaviour of W in H-mode plasmas with several ITER-like characteristics including: plasma density peaking, low/no central source of neutral, electron dominant heating (with  $T_e/T_i < 2$ ) and low core plasma toroidal rotation ( $M_D < 0.1$ ).

The major result obtained in these experiments is that under such conditions no strong core W peaking is typically obtained. Exceptions are cases with strong MHD activity or when very high H minority concentrations are used for ICRH heating. This experimental result can be explained by W transport being dominated by anomalous W transport with a large diffusive component across the plasma cross section in the range  $0.3 < \rho < \rho_{ETB}$  (where ETB is the inner point of the edge transport barrier), while inside  $\rho < 0.3$  W transport is better described by neoclassical transport, which is in good agreement with finding in other experiments [Angioni 2014a]. On the other hand and contrary to these other experiments, the scale lengths for the plasma temperature and density inside  $\rho < 0.3$  are such that core neoclassical transport of W does not have a strong inward pinch and, thus, W does not accumulate in the plasma core. Here the fact that these plasmas are ITER-like in terms of the core source of neutrals (i.e. no/very low source of neutrals provided by the NBI+RF heating systems) is key to prevent the excessive core density peaking found in NBI dominated experiments that show strong W accumulation [Angioni 2014a].

In addition, the timescales for W diffusion inwards from the anomalous transport dominated zone into the central plasma region ( $a_p \leq 0.3 a$ ) where anomalous transport is negligible are well described by neoclassical transport expectations for the Alcator C-Mod plasmas with very low plasma rotation. This provides a solid basis for the extrapolation of this timescale to ITER. The W transport timescales found in Alcator C-Mod can be extrapolated to ITER by taking into account that:

$$\frac{\tau_W^{ITER}}{\tau_W^{C-Mod}} = \frac{a_{p-ITER}^2}{a_{p-C-Mod}^2} \frac{D_{C-Mod}^{neoc.}}{D_{ITER}^{neoc.}} \quad (6)$$

which corresponds to  $\tau_W^{ITER} = 3.5$  s for  $\tau_W^{C-Mod} = 15$  ms, assuming that the ratio  $a_p/a$  is similar in Alcator C-Mod and ITER, which is well justified on the basis of the ITER modelling results in Fig. 2 and Alcator C-Mod experimental observations in Fig. 7. From this large ratio between ITER and Alcator C-Mod a factor of  $\sim 80$  comes from the device size and the remaining factor of 3 from the difference in neoclassical transport diffusion coefficients between the two devices (note that the magnetic field in these Alcator C-Mod discharges is virtually the same of ITER  $Q_{DT} = 10$  plasmas). This shows that W accumulation in ITER, if it were to occur, can be detected well in advance of when it may cause excessive W radiation and affect plasma performance. A timescale of 3.5 s allows core heating to be applied to arrest such possible W peaking well in advance of the point when it has a detrimental effect on plasma performance, as shown in the ITER modelling results of Sect. 2. Last but not least, these Alcator C-Mod experiments results show that, although sawtooth modulate the W density in the central plasma region, this effect is not required to explain the lack of W peaking in the experiments. This implies that the lack of sawtooth-averaged W density peaking in these ITER-like H-mode plasmas in Alcator C-Mod is not driven by the repetitive flattening of the W density profile by the sawteeth but by the fact that inter-sawtooth central W transport does not lead to strong central W density peaking, in agreement with similar recent observations at JET [Goniche 2014, Graves 2014], which is a key result for ITER.

The efficiency of sawteeth to expel W from the core plasma is determined by the ratio of the time that it takes W to diffuse/convect into the core plasma ( $\tau_W^{core}$ ) to the sawtooth repetition period ( $\tau_{sawtooth}$ ). In the Alcator C-Mod discharges studied, the typical value of  $\tau_W^{core}$  is  $\sim 10$  ms, as discussed above, while the typical sawtooth period is  $\tau_{sawtooth} \sim 10$  ms (see Fig. 9 for an example). In these circumstances the effectiveness of sawteeth to expel W from the core is potentially very high, as  $\tau_W^{core}/\tau_{sawtooth}|_{C-Mod} \sim 1$ . This means that, even if W would strongly peak in the core plasma between sawteeth in Alcator C-Mod, the sawtooth averaged W density peaking would be much lower (typically  $\sim 1/2$  of the peaking before sawteeth). On the contrary, for ITER the expected sawtooth period for  $Q_{DT} = 10$  plasmas is expected to be very long  $\tau_{sawtooth} \sim 30-40$  s [Hender 2007], due to stabilizing effects of fast particles (produced by the additional heating systems and the alpha particles themselves) on the MHD sawtooth trigger. This should be compared with the typical  $\tau_W^{core} \sim 3.5$  s leading to  $\tau_W^{core}/\tau_{sawtooth}|_{ITER} \sim 0.1$ . In ITER, therefore, the effectiveness of sawteeth to expel W from the

core is expected to be negligible and intra-sawtooth transport dominates the core peaking of  $W$ . In this respect, it is important the experimental confirmation that for ITER-like H-mode plasmas in Alcator C-Mod it is the intra-sawtooth transport which leads to flat core  $W$  profiles and that these flat profiles are not the consequence of sawtooth activity, as the latter would not extrapolate to ITER.

Overall, the Alcator C-Mod experiments show that the key modelling assumptions and modelling results obtained for ITER in Sect. 2 are well based on the experimental results from ITER-like H-mode plasmas in Alcator C-Mod. Thus the positive picture regarding the lack of strong  $W$  peaking in ITER reference  $Q_{DT}=10$  plasmas is well justified on present understanding. In this respect, the fact that the ITER NBI heating system provides a source of particles in the core plasma with a density rate two to three orders of magnitude lower than in present NBI-dominated experiments is key for this positive picture regarding core  $W$  transport in ITER; which is well justified by the RF heated Alcator C-Mod experimental results presented here. In addition, ITER modelling and the Alcator C-Mod experiments show that the expected density peaking from anomalous transport in the region  $0.3 < \rho < \rho_{ETB}$ , which can be beneficial to improve fusion performance in ITER, does not have a negative impact regarding  $W$  peaking in the  $0.3 < \rho < \rho_{ETB}$  region because  $W$  transport in that region is dominated by diffusive anomalous transport with a large diffusion coefficient in the modelled ITER plasmas. This is in excellent agreement with the observations of  $W$  penetration (following  $W$  LBOs) into the core plasma of the Alcator C-Mod ITER-like H-modes with ITER-like density peaking and thus a robust prediction for ITER.

While the results obtained in these Alcator C-Mod experiments are very encouraging regarding the expected features of core  $W$  transport in ITER, there remain open questions regarding the latter and also on the extrapolability of the results of the Alcator C-Mod experiments to ITER. One such question concerns the role of fast particles on neoclassical  $W$  transport in Alcator C-Mod and expectations for ITER. Fast particle species and energy distributions will be very different in ITER (alpha particles with  $\sim 3.5$  MeV energies, 1 MeV fast D ions from NBI, fast T, H or  $\text{He}^3$  from ICRH heating,...) from those in Alcator C-Mod (H-minority accelerated ions). Present understanding shows that fast ions can influence  $W$  density peaking in the central plasma due to friction between high energy ICRH minority ions and  $W$  ions [Casson 2014]. This could change the  $W$  density profiles in the central plasma region in ITER with respect to the modelling based on the thermal plasma parameters alone shown in Sect. 2. Initial results from Alcator C-Mod ITER-like H-mode experiments indicate that  $W$  peaking could be higher than what is expected from the thermal plasma parameters for

some fast particle distributions, such as those obtained with high percentage of hydrogen minority. Another open question concerns the lower equipartition and higher  $T_e/T_i$  ratio found in Alcator C-Mod with respect to ITER, given the different degrees of stiffness of the electron and ion temperature profiles and the different effects of pushing these two temperature profiles against their stiff limits on the density profiles seen in Alcator C-Mod experiments and in ITER modelling. Further experiments and modelling of the existing experimental results presented here are required to make progress in these two areas. This could include additional experiments in Alcator C-Mod by varying the minority concentration level, ICRH resonance location, electron to ion heating ratio by using  $\text{He}^3$  minority as foreseen for ITER, etc.

Finally, another area where more analysis, experiments and modelling are required is the one regarding the characterization of the processes leading to the expulsion of W outside the ETB in ITER-like H-mode plasmas, which has not been discussed in this paper. In conditions in which no strong W peaking takes place this is regulated by the exhaust of W through the ETB, which for the Alcator C-Mod plasmas studies here is related to the edge turbulent transport associated with the EDA regime (and with the effective transport by controlled ELMs in ITER) and with the underlying neoclassical transport in the ETB region. The results obtained in these Alcator C-Mod experiments show that the typical W confinement time in the plasma (i.e. the typical timescale for the central W emission to decay after the LBO) can vary from  $\sim 50$  to 200 ms when the LBO does not trigger an H-L transition, as shown in Fig. 11. It remains to be understood whether changes of edge turbulent transport or of the neoclassical transport in the ETB with the variation of plasma parameters explored dominate the observed changes on the W confinement time and how these physics processes extrapolate to ITER.

### **Acknowledgements**

The authors would like to thank the Alcator C-Mod operations staff, particularly S. Wolfe, for their contribution to the success of the experiments reported in this paper, C. Angioni and P. Mantica for helpful discussions on the ITER W modelling and M. O'Mullane for providing atomic data required for the interpretation of the soft-X ray signals. This work was supported by the US Department of Energy Agreement DE-FC02-99ER54512.

### **Disclaimer**

The views and opinions expressed herein do not necessarily reflect those of the ITER Organization.

## 6. References.

- [Angioni 2007] C. Angioni, H. Weisen, O.J.W.F. Kardaun, M. Maslov, A. Zabolotsky, C. Fuchs, L. Garzotti, C. Giroud, B. Kurzan, P. Mantica, A.G. Peeters, J. Stober and the ASDEX Upgrade Team and contributors to the EFDA-JET Workprogramme, Nucl. Fusion **47** (2007) 1326.
- [Angioni 2014a] C. Angioni, P. Mantica, T. Pütterich, M. Valisa, M. Baruzzo, E.A. Belli, P. Belo, F.J. Casson, C. Challis, P. Drewelow, C. Giroud, N. Hawkes, T.C. Hender, J. Hobirk, T. Koskela, L. Lauro Taroni, C.F. Maggi, J. Mlynar, T. Odstreil, M.L. Reinke, M. Romanelli and JET EFDA Contributors, Nucl. Fusion **54** (2014) 1083028.
- [Angioni 2014b] C. Angioni and P. Helander, Plasma Phys. Control. Fusion **56** (2014) 124001.
- [Basse 2007] N. P. Basse, A. Dominguez, E. M. Edlund, C. L. Fiore, R. S. Granetz, A. E. Hubbard, J. W. Hughes, I. H. Hutchinson, J. H. Irby, B. LaBombard, L. Lin, Y. Lin, B. Lipschultz, J. E. Liptac, E. S. Marmor, D. A. Mossessian, R. R. Parker, M. Porkolab, J. E. Rice, J. A. Snipes, V. Tang, J. L. Terry, S. M. Wolfe, S. J. Wukitch, K. Zhurovich, R. V. Bravenec, P. E. Phillips, W. L. Rowan, G. J. Kramer, G. Schilling, S. D. Scott and S. J. Zweben, Fusion Sci. Technol. **51**(2007) 476
- [Campbell 2012] D. J. Campbell for the ITER Organization, Domestic Agencies and ITER collaborators, in Fusion Energy 2012 (Proc. 24<sup>th</sup> Int. Conf. San Diego), Paper ITR/P1-18.
- [Casson 2014] F.J. Casson, C. Angioni, E.A. Belli, R. Bilato, P. Mantica, T. Odstreil, T. Puetterich, M. Valisa, L. Garzotti, C. Giroud, J. Hobirk, C.F. Maggi, J. Mlynar, M.L. Reinke, JET EFDA contributors and the ASDEX-Upgrade team, 41<sup>st</sup> European Physical Society Conference on Plasma Physics, Berlin, Germany, 2014, to be published in Plasma Phys. Control. Fusion. (<http://arxiv.org/abs/1407.1191>).
- [de Vries 2012] P. C. de Vries, G. Arnoux, A. Huber, J. Flanagan, M. Lehnen, V. Riccardo, C. Reux, S. Jachmich, C. Lowry, G. Calabro, D. Frigione, M. Tsalias, N. Hartmann, S. Brezinsek, M. Clever, D. Douai, M. Groth, T. C. Hender, E. Hodille, E. Joffrin, U. Kruezi, G. F. Matthews, J. Morris, R. Neu, V. Philipps, G. Sergienko, M. Sertoli and JET EFDA contributors, Plasma Phys. Control. Fusion **54** (2012) 124032.
- [Dux 1999] R. Dux, A.G. Peeters, A. Gude, A. Kallenbach, R. Neu and ASDEX Upgrade Team, Nucl. Fusion **39** (1999) 11.
- [Dux 2003] R. Dux, R. Neu, A. G. Peeters, G. Pereverzev, A. Mück, F. Ryter, J. Stober and ASDEX Upgrade Team, Plasma Phys. Control. Fusion **45** (2003) 1815.
- [Dux 2006] R. Dux, IPP Report, IPP 10/30, 2006
- [Evans 2006] T.E. Evans, R.A. Moyer, K.H. Burrell, M.E. Fenstermacher, I. Joseph, A.W. Leonard, T.H. Osborne, G.D. Porter, M.J. Schaffer, P.B. Snyder, P.R. Thomas, J.G. Watkins and W.P. West, Nature Physics **2** (2006) 419.
- [Federici 2003] G. Federici, A. Loarte and G. Strohmayer, Plasma Phys. Control. Fusion (2003) **45** 1523.
- [Goniche 2014] M. Goniche, E. Lerche, P. Jacquet, D. Van Eester, V. Bobkov, S. Brezinsek, L. Colas, A. Czarnecka, P. Drewelow, R. Dumont, N. Fedorczak, C. Giroud, M. Graham, J.P. Graves, I. Monakhov, P. Monier-Garbet, C. Noble, T. Pütterich, F. Rimini, M. Valisa and JET EFDA contributors, 41<sup>st</sup> European Physical Society Conference on Plasma Physics, Berlin, Germany, 2014, paper O4.129.

[Graves 2014] J. P. Graves, M. Lennholm, I. T. Chapman, E. Lerche, M. Reich, V. Bobkov, R. Dumont, D. Van Eester, J. Faustin, M. Goniche, P. Jacquet, T. Johnson, Y. Liu, T. Nicolas, S. Tholerus, T. Blackman, I. S. Carvalho, R. Felton, V. Kiptily, I. Monakhov, M. F. F. Nave, C. Sozzi, M. Tsalas and JET EFDA Contributors, 41<sup>st</sup> European Physical Society Conference on Plasma Physics, Berlin, Germany, 2014, paper I5.120.

[Greenwald 1999] M. Greenwald, R. Boivin, P. Bonoli, R. Budny, C. Fiore, J. Goetz, R. Granetz, A. Hubbard, I. Hutchinson, J. Irby, B. LaBombard, Y. Lin, B. Lipschultz, E. Marmar, A. Mazurenko, D. Mossessian, T. Sunn Pedersen, C. S. Pitcher, M. Porkolab, J. Rice, W. Rowan, J. Snipes, G. Schilling, Y. Takase, J. Terry, S. Wolfe, J. Weaver, B. Welch, and S. Wukitch, *Phys. Plasmas* **6** (1999) 1943.

[Greenwald 2007] M. Greenwald, C. Angioni, J.W. Hughes, J. Terry and H. Weisen, *Nucl. Fusion* **47** (2007) L26.

[Hender 2007] T.C. Hender, J.C. Wesley, J. Bialek, A. Bondeson, A.H. Boozer, R.J. Buttery, A. Garofalo, T.P. Goodman, R.S. Granetz, Y. Gribov, O. Gruber, M. Gryaznevich, G. Giruzzi, S. Günter, N. Hayashi, P. Helander, C.C. Hegna, D.F. Howell, D.A. Humphreys, G.T.A. Huysmans, A.W. Hyatt, A. Isayama, S.C. Jardin, Y. Kawano, A. Kellman, C. Kessel, H.R. Koslowski, R.J. La Haye, E. Lazzaro, Y.Q. Liu, V. Lukash, J. Manickam, S. Medvedev, V. Mertens, S.V. Mirnov, Y. Nakamura, G. Navratil, M. Okabayashi, T. Ozeki, R. Paccagnella, G. Pautasso, F. Porcelli, V.D. Pustovitov, V. Riccardo, M. Sato, O. Sauter, M.J. Schaffer, M. Shimada, P. Sonato, E.J. Strait, M. Sugihara, M. Takechi, A.D. Turnbull, E. Westerhof, D.G. Whyte, R. Yoshino, H. Zohm and the ITPA MHD, Disruption and Magnetic Control Topical Group, *Nucl. Fusion* **47** (2007) S128.

[Houlberg 1997] W. A. Houlberg, K. C. Shaing, S. P. Hirshman and M. C. Zarnstorff, *Phys. Plasmas* **4** (1997) 3230.

[Howard 2011] N. T. Howard, M. Greenwald and J. E. Rice, *Rev. Sci. Instrum.* **82** (2011) 033512

[Hughes 2007] J.W. Hughes, B. LaBombard, J. Terry, A. Hubbard and B. Lipschultz, *Nucl. Fusion* **47** (2007) 1057.

[Hutchinson 1994] I. H. Hutchinson, R. Boivin, F. Bombarda, P. Bonoli, S. Fairfax, C. Fiore, J. Goetz, S. Golovato, R. Granetz, M. Greenwald, S. Horne, A. Hubbard, J. Irby, B. LaBombard, B. Lipschultz, E. Marmar, G. McCracken, M. Porkolab, J. Rice, J. Snipes, Y. Takase, J. Terry, S. Wolfe, C. Christensen, D. Garnier, M. Graf, T. Hsu, T. Luke, M. May, A. Niemczewski, G. Tinios, J. Schachter and J. Urbahn, *Phys. Plasmas* **1** (1994) 1511.

[IPB 1999] ITER Physics Expert Group on Confinement and Transport, ITER Physics Expert Group on Confinement Modelling and Database and ITER Physics Basis Editors, *Nucl. Fusion* **39** (1999) 2175.

[Kallenbach 2005] A. Kallenbach, R. Neu, R. Dux, H.-U. Fahrbach, J. C. Fuchs, L. Giannone, O. Gruber, A. Herrmann, P.T. Lang, B. Lipschultz, C.F. Maggi, J. Neuhauser, V. Philipps, T. Pütterich, V. Rohde, J. Roth, G. Sergienko, A. Sips and ASDEX Upgrade Team, *Plasma Phys. Control. Fusion* **47** (2005) B207.

[Leonov 2005] V.M. Leonov and V.E. Zhogolev, *Plasma Phys. Control. Fusion* **47** (2005) 903.

[Loarte 2014] A. Loarte, G. Huijsmans, S. Futatani, L.R. Baylor, T.E. Evans, D. M. Orlov, O. Schmitz, M. Becoulet, P. Cahyna, Y. Gribov, A. Kavin, A. Sashala Naik, D.J. Campbell, T.

Casper, E. Daly, H. Frerichs, A. Kischner, R. Laengner, S. Lisgo, R.A. Pitts, G. Saibene and A. Wingen, Nucl. Fusion **54** (2014) 033007.

[Mantica 2014] P. Mantica, C. Angioni, F.J. Casson, T. Pütterich, M. Valisa, M. Baruzzo, P.C. da Silva Aresta Belo, I. Coffey, P. Drewelow, C. Giroud, N.C. Hawkes, T.C. Hender, T. Koskela, L. Lauro Taroni, E. Lerche, C.F. Maggi, J.Mlynar, M. O'Mullane, M.E. Puiatti, M.L. Reinke, M. Romanelli and JET EFDA contributors, 41<sup>st</sup> European Physical Society Conference on Plasma Physics, Berlin, Germany, 2014, paper P1.017.

[Marmar 2007] E. S. Marmar and Alcator C-Mod Group, Fusion Sci. Technol. **51** (2007) 261.

[Neu 2002] R. Neu, R. Dux, A. Geier, A. Kallenbach, R. Pugno, V. Rohde, D. Bolshukhin, J.C. Fuchs, O. Gehre, O. Gruber, J. Hobirk, M. Kaufmann, K. Krieger, M. Laux, C. Maggi, H. Murmann, J. Neuhauser, F. Ryter, A.C.C. Sips, A. Stäbler, J. Stober, W. Suttrop, H. Zohm and the ASDEX Upgrade Team, Plasma Phys. Control. Fusion **44** (2002) 811.

[Parail 2013] V. Parail, R. Albanese, R. Ambrosino, J.-F. Artaud, K. Besseghir, M. Cavinato, G. Corrigan, J. Garcia, L. Garzotti, Y. Gribov, F. Imbeaux, F. Koechl, C.V. Labate, J. Lister, X. Litaudon, A. Loarte, P. Maget, M. Mattei, D. McDonald, E. Nardon, G. Saibene, R. Sartori and J. Urban, Nucl. Fusion **53** (2013) 113002.

[Pereverzev 2002] G. V. Pereverzev and P. N. Yushmanov, ASTRA - Automated System for Transport Analysis, Report IPP 5/98.

[Pütterich 2010] T. Pütterich, R. Neu, R. Dux, A.D. Whiteford, M.G. O'Mullane, H.P. Summers and the ASDEX Upgrade Team, Nucl. Fusion **50** (2010) 025012.

[Pütterich 2011] T. Pütterich, R. Dux, M.A. Janzer, R.M. McDermott and the ASDEX Upgrade Team, J. Nucl. Mat. **415** (2011) S334.

[Pütterich 2013] T. Pütterich, R. Dux, R. Neu, M. Bernert, M.N.A. Beurskens, V. Bobkov, S. Brezinsek, C. Challis, J.W. Coenen, I. Coffey, A. Czarnecka, C. Giroud, P. Jacquet, E. Joffrin, A. Kallenbach, M. Lehnen, E. Lerche, E. de la Luna, S. Marsen, G. Matthews, M.-L. Mayoral, R.M. McDermott, A. Meigs, J. Mlynar, M. Sertoli, G. van Rooij, the ASDEX Upgrade Team and JET EFDA Contributors, Plasma Phys. Control. Fusion **55** (2013) 124036

[Rice 1997] J. E. Rice, J. L. Terry, J. A. Goetz, Y. Wang, E. S. Marmar, M. Greenwald, I. Hutchinson, Y. Takase, S. Wolfe, H. Ohikawa and A. Hubbard, Phys. Plasmas **4** (1997) 1605.

[Rice 2000] J. E. Rice, J. A. Goetz, R. S. Granetz, M. J. Greenwald, A. E. Hubbard, I. H. Hutchinson, E. S. Marmar, D. Mossessian, T. Sunn Pedersen, J. A. Snipes, J. L. Terry and S. M. Wolfe, Phys. Plasmas **7** (2000) 1825.

[Rice 2007] J. E. Rice, J. L. Terry, E. S. Marmar, R. S. Granetz, M. J. Greenwald, A. E. Hubbard, J. H. Irby, S. M. Wolfe and T. Sunn Pedersen, Fusion Sci. Technol. **51** (2007) 357.

[Reinke 2008] M.L. Reinke and I.H. Hutchinson, Rev. Sci. Instrum. **79** (2008) 10F306.

[Reinke 2010] M.L. Reinke, P. Beiersdorfer, N.T. Howard, E.W. Magee, Y. Podpaly, J.E. Rice and J.L. Terry, Rev. Sci. Instrum. **81** (2010) 10D736. [Reinke 2012] M.L. Reinke, Y.A. Podpaly, M. Bitter, I.H. Hutchinson, J.E. Rice, L. Delgado-Aparicio, C. Gao, M. Greenwald, K. Hill, N.T. Howard, A. Hubbard, J.W. Hughes, N. Pablant, A.E. White and S.M. Wolfe, Rev. Sci. Instrum. **83** (2012) 113501.

[Snyder 2011] P.B. Snyder, R.J. Groebner, J.W. Hughes, T.H. Osborne, M. Beurskens, A.W. Leonard, H.R. Wilson and X.Q. Xu, Nucl. Fusion **51** (2011) 103016.

[Sunn Pedersen 2000] T. Sunn Pedersen, R.S. Granetz, A.E. Hubbard, I.H. Hutchinson, E.S. Marmar, J.E. Rice and J. Terry, Nucl. Fusion **40** (2000) 1795.



[Waltz 1997] R.E. Waltz, G.M. Staebler, W. Dorland, G.W. Hammett, M. Kotschenreuther and J.A. Konings, Phys. Plasmas **4** (1997) 2482.

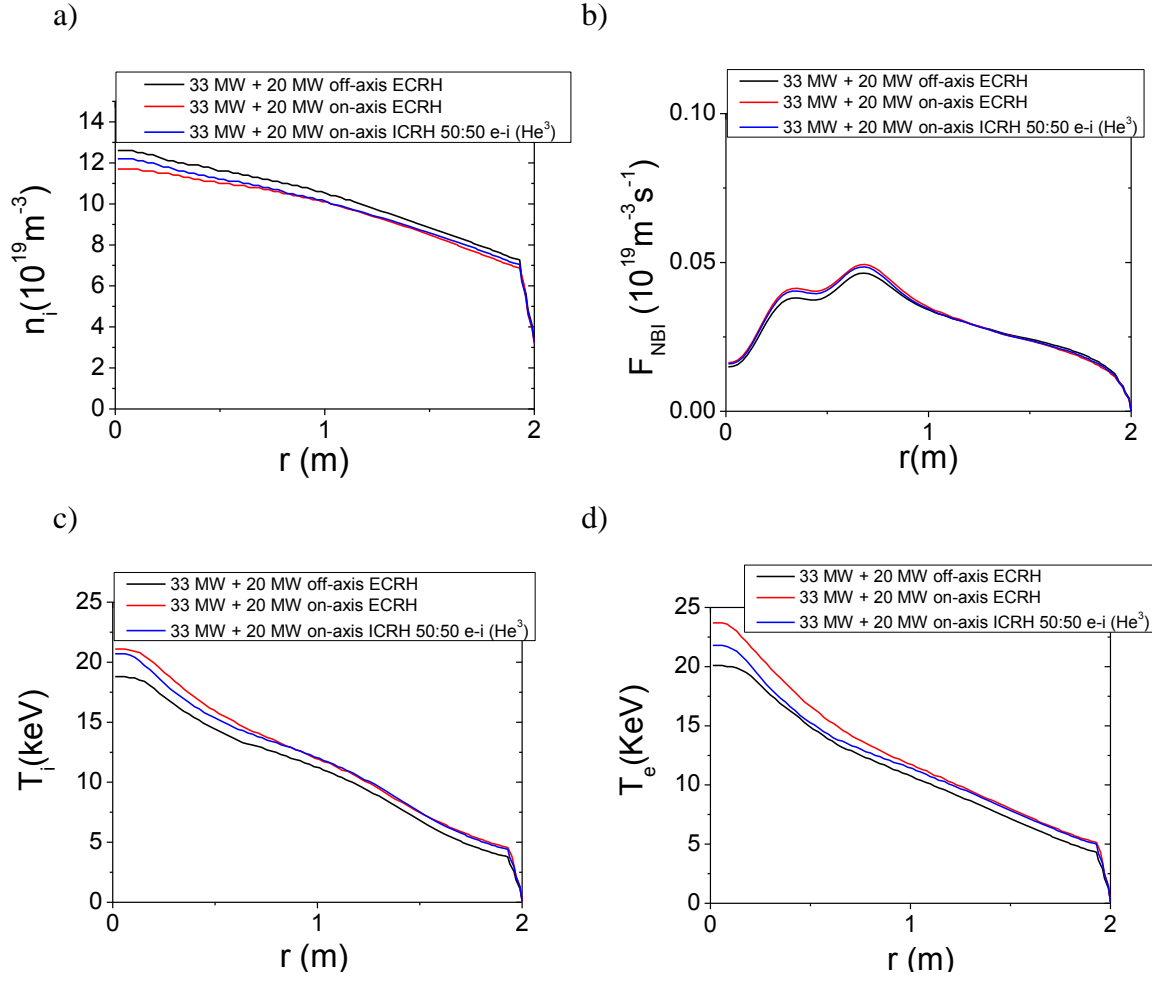


Figure 1. Results of ASTRA simulations for ITER 15 MA/5.3 T  $Q_{DT}=10$  plasma with different heating schemes (33 MA of NBI + 20 MW of off axis or on axis ECRH and 33 MA of NBI + 20 MW of on axis ICRH with  $\text{He}^3$  minority to provide maximum ion heating): a) ion density profile versus minor radius, b) NBI neutral source versus minor radius, c) ion temperature profiles versus minor radius and d) electron temperature profile versus minor radius.

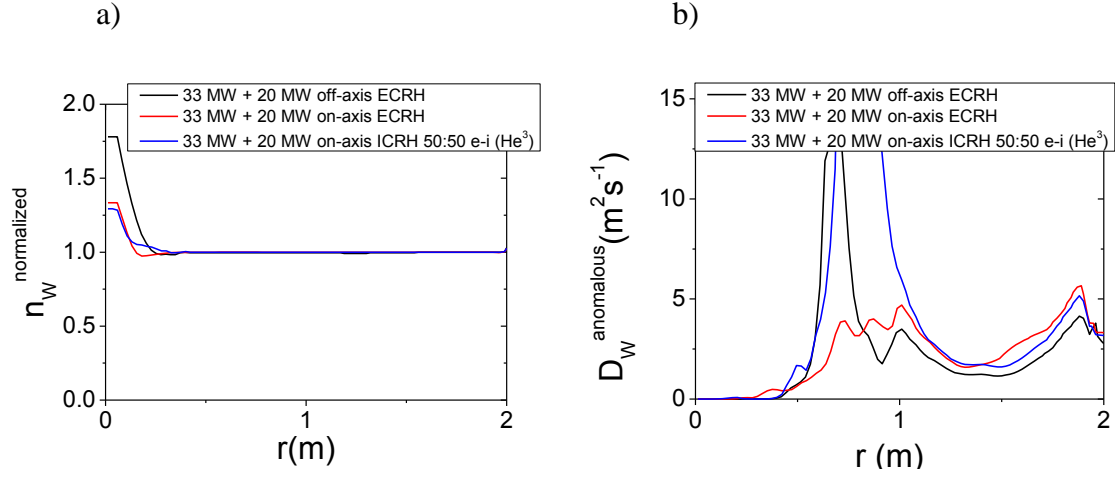


Figure 2. Results of ASTRA simulations for ITER 15 MA/5.3 T  $Q_{DT}=10$  plasma with different heating schemes (33 MA of NBI + 20 MW of off axis or on axis ECRH and 33 MA of NBI + 20 MW of on axis ICRH with  $He^3$  minority to provide maximum ion heating): a) normalized W density profile versus minor radius, b) anomalous diffusion coefficient for W transport as evaluated by the GLF23 transport model versus minor radius.

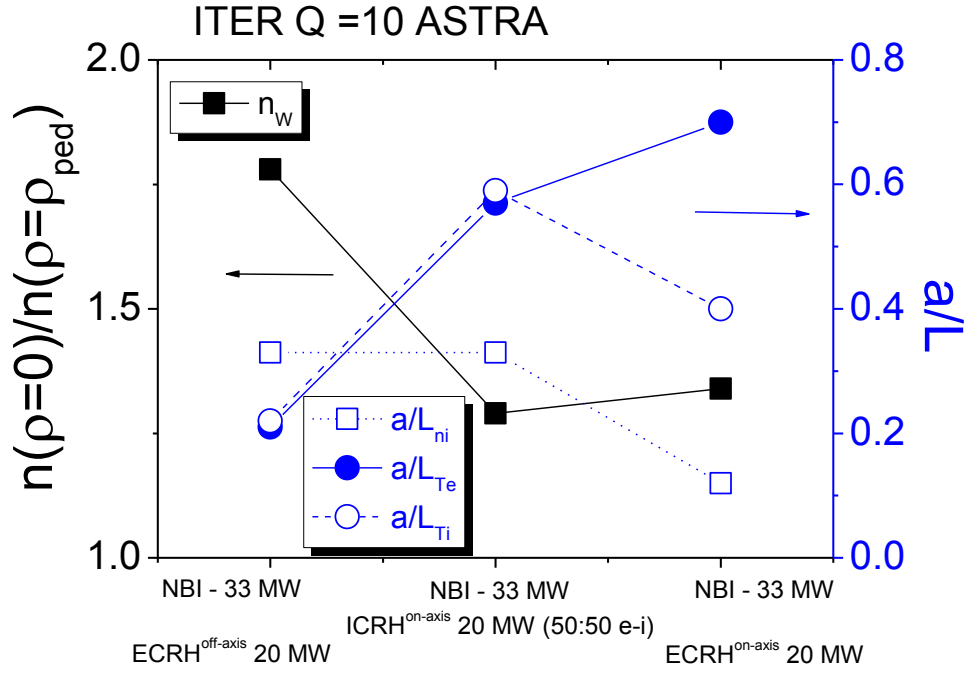


Figure 3. Results of ASTRA simulations for ITER 15 MA/5.3 T  $Q_{DT}=10$  plasma with different heating schemes (33 MA of NBI + 20 MW of off axis or on axis ECRH and 33 MA of NBI + 20 MW of on axis ICRH with  $He^3$  minority to provide maximum ion heating): Left axis) central W density peaking, Right axis) inversed normalized (to the minor radius) scale lengths for the ion density and ion and electron temperatures at  $r \sim 0.3$  m.

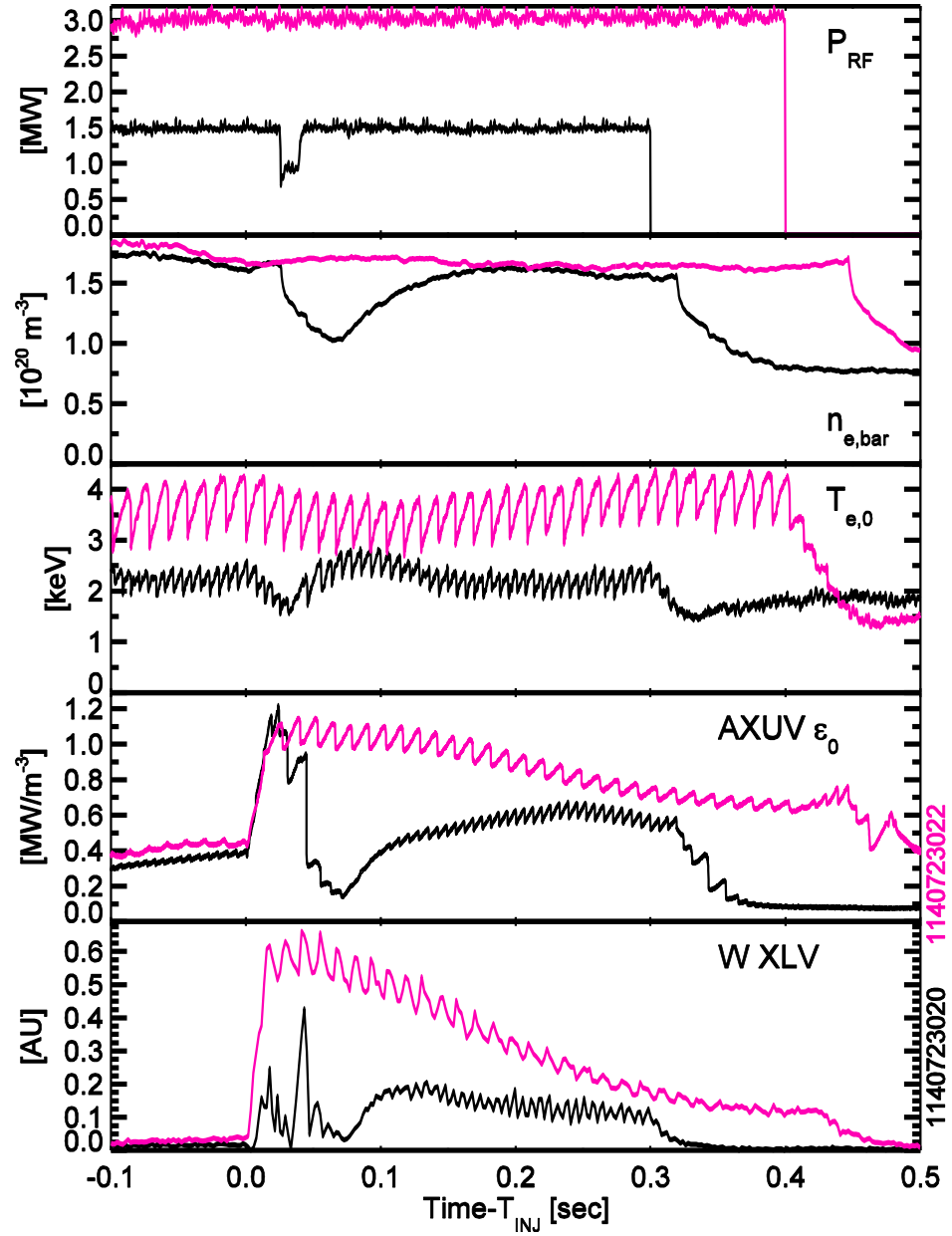


Figure 4. Measurements of plasma parameters and W emission in two typical Alcator C-Mod discharges with W LBO with  $I_p = 0.52$  MA. From top to bottom: coupled ICRH power, line average density measured by the interferometer, central electron temperature measured by ECE, central extreme ultraviolet emission, and line-integrated emission from  $W^{44+}$ , a near-core charge state.

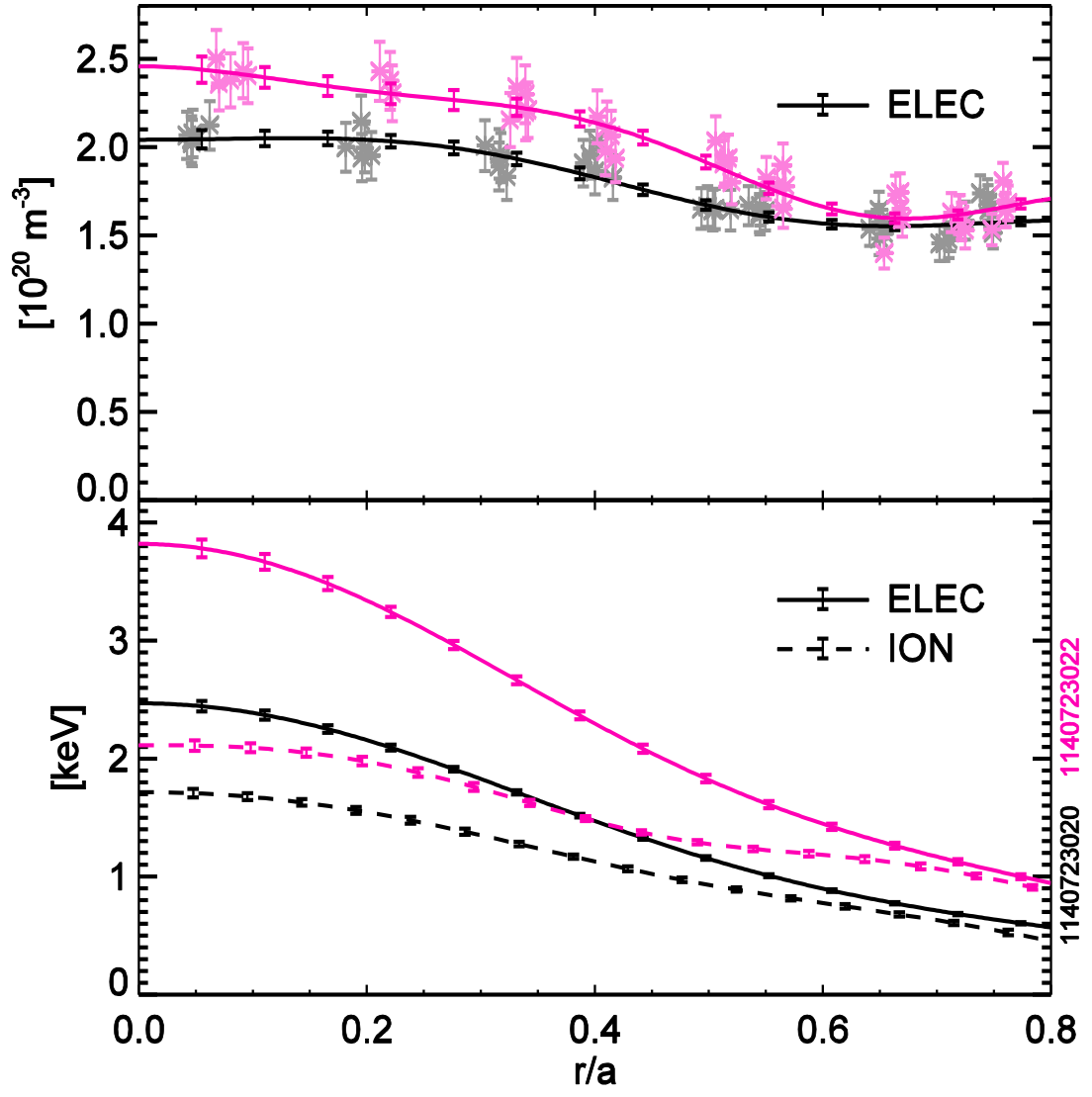


Figure 5. Measurements of electron plasma density (top) and electron and ion temperatures (bottom) for the discharges in Fig. 4 (black  $P_{\text{ICRH}} = 1.5$  MW and magenta  $P_{\text{ICRH}} = 3.0$  MW).

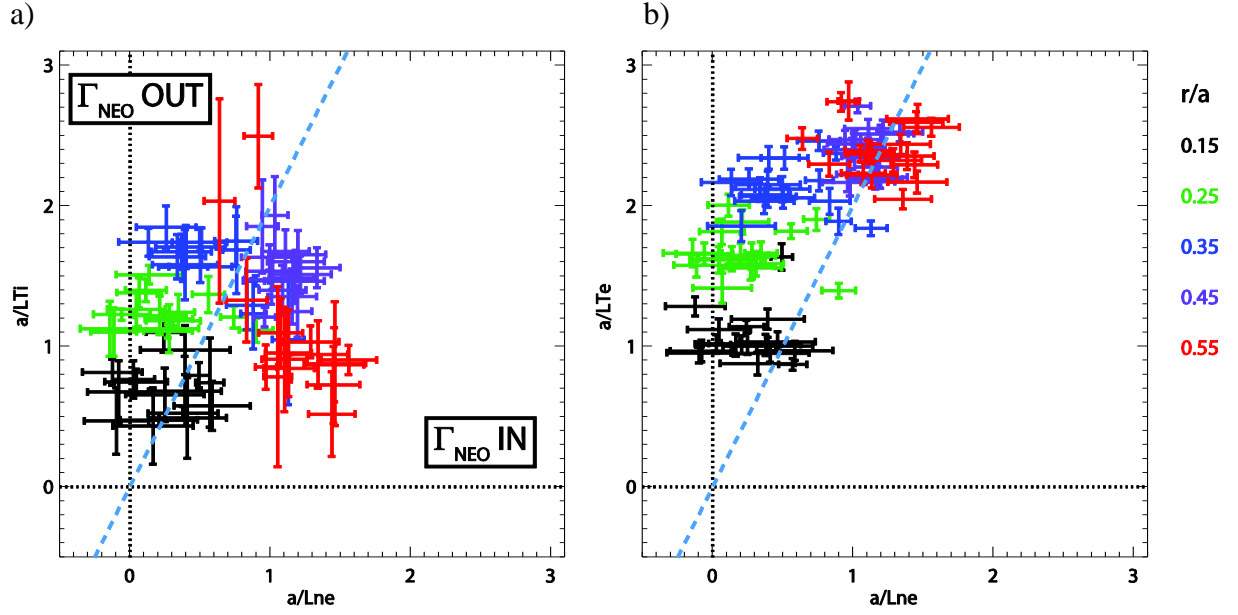


Figure 6. Measurements of the ion (a) and electron temperature (b) normalized inverse scale lengths versus electron density inverse scale lengths for a set of C-Mod discharges at various radial locations across the plasma core within  $0.15 \leq \rho \leq 0.55$ . The line for which  $a/L_{Ti,e} = a/(2L_{ne})$  determining (when ion parameters are considered) the direction of neoclassical transport for W according to Eq. 1 is shown for reference.

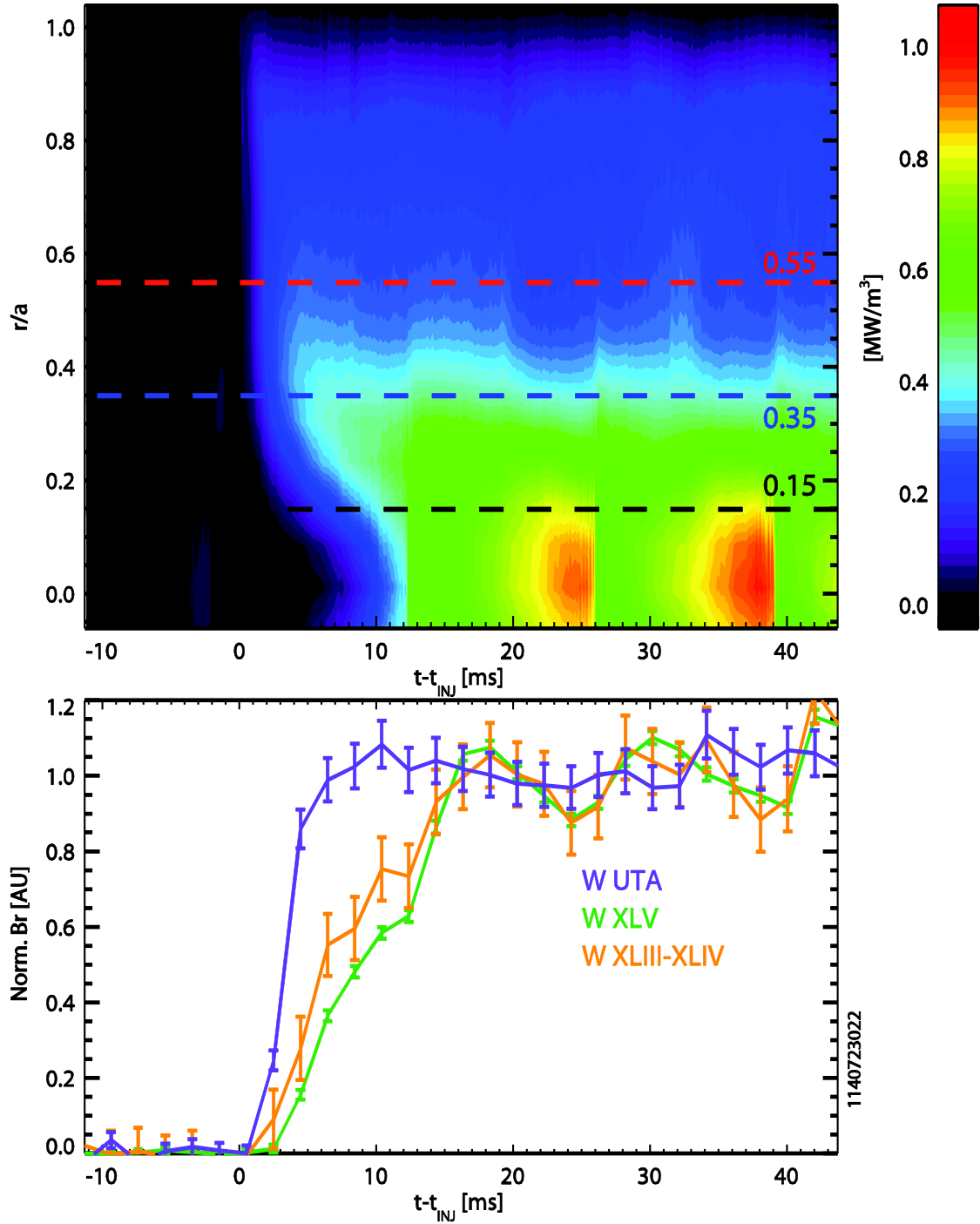


Figure 7. Measured time evolution of the AXUV diode emission (top) and spectroscopic line emission (bottom) following W injection by LBO ( $t = 0$  ms is the LBO time) in an ITER-like Alcator C-Mod H-mode plasma. A fast inward propagation of the W emission up to  $\rho = 0.3$  takes place within few ms; further penetration to  $\rho = 0.0$  requires typically 10 ms or more. The modulation of the W emission signal after  $t = 20$  ms for  $\rho \leq 0.4$  is due to sawteeth.



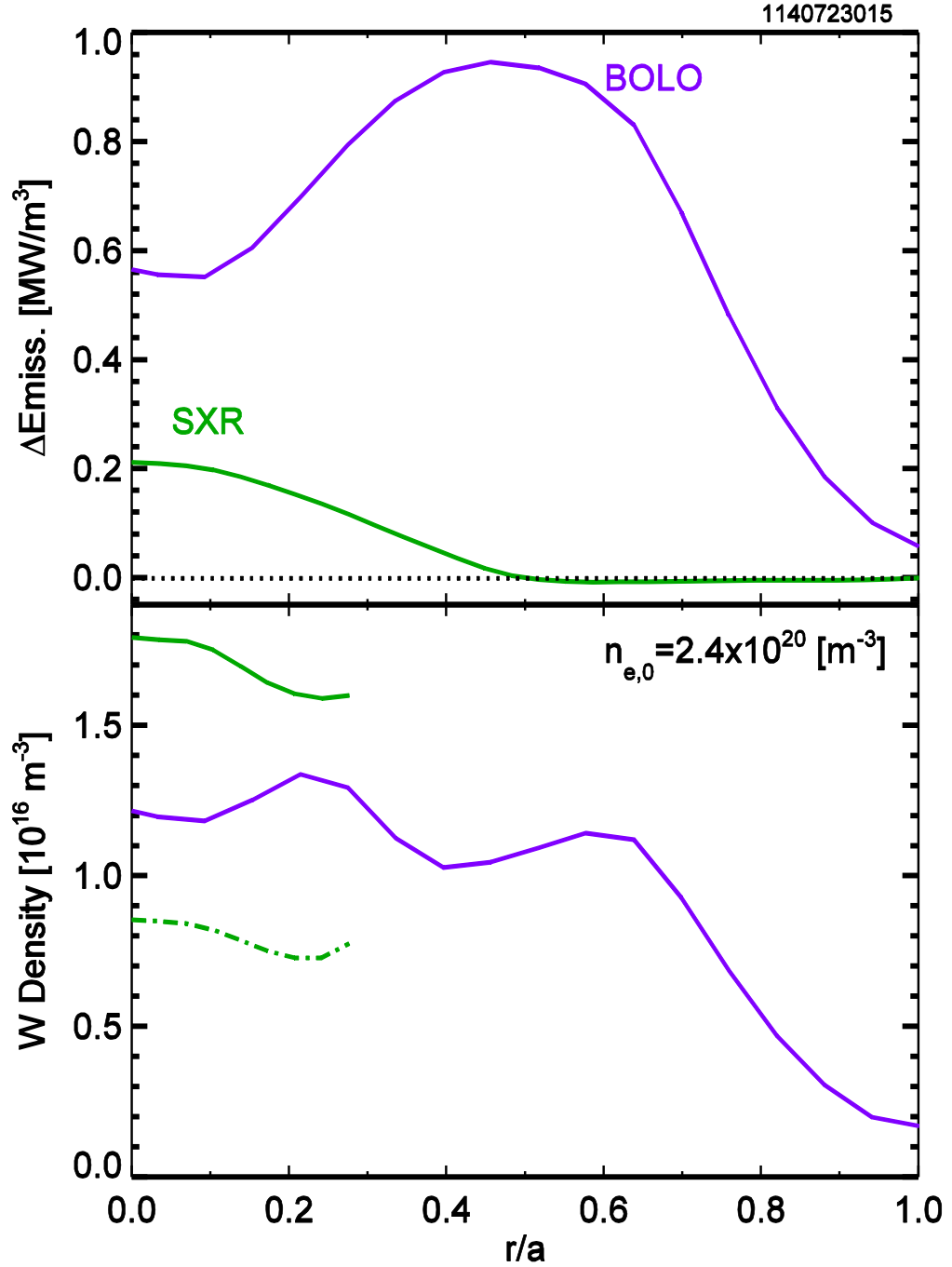


Figure 8. Top) Measurements of the increased radiated and soft X-ray power densities (through a 50  $\mu\text{m}$  Be filter) following W LBO in an ITER-like Alcator C-Mod H-mode plasma. Bottom) Estimated W density from the radiated and soft X-ray power densities from the measured plasma density and temperature profiles and the expected radiation efficiency of W in these conditions. Full lines and dashed-lines correspond to estimates based on the different sets of atomic modelling data for the SXR emission.

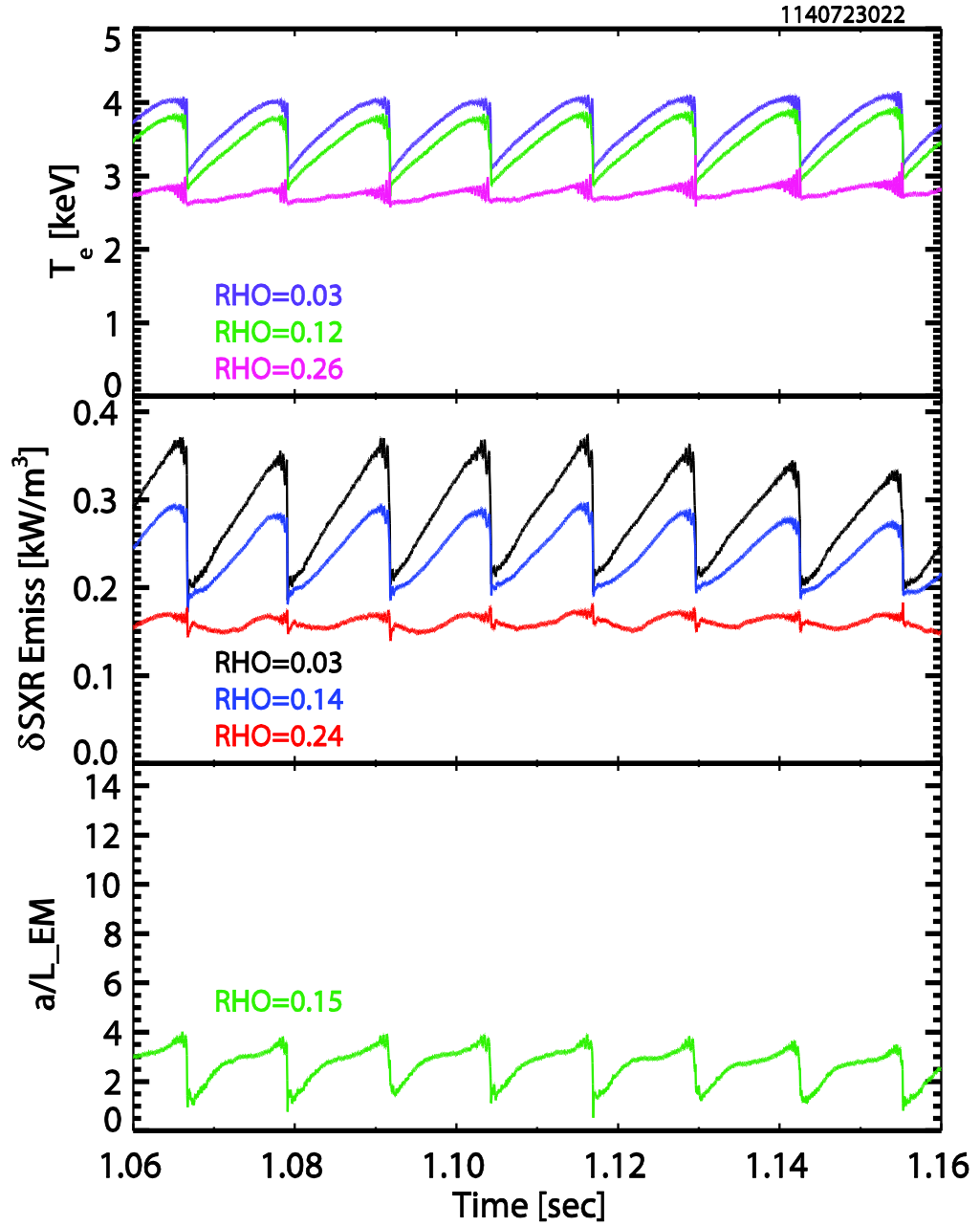


Figure 9. (Top) Measurements of the electron temperature evolution between sawteeth up to the inversion radius ( $\rho \sim 0.25$ ) for an ITER-like H-mode plasma in Alcator C-Mod following W LBO injection. (Middle) Measurements of the soft X-ray power density (through a 50  $\mu m$  Be filter) in an ITER-like Alcator C-Mod H-mode plasma following W LBO injection. (Bottom) Calculated emissivity gradient scale length at  $\rho = 0.15$ .

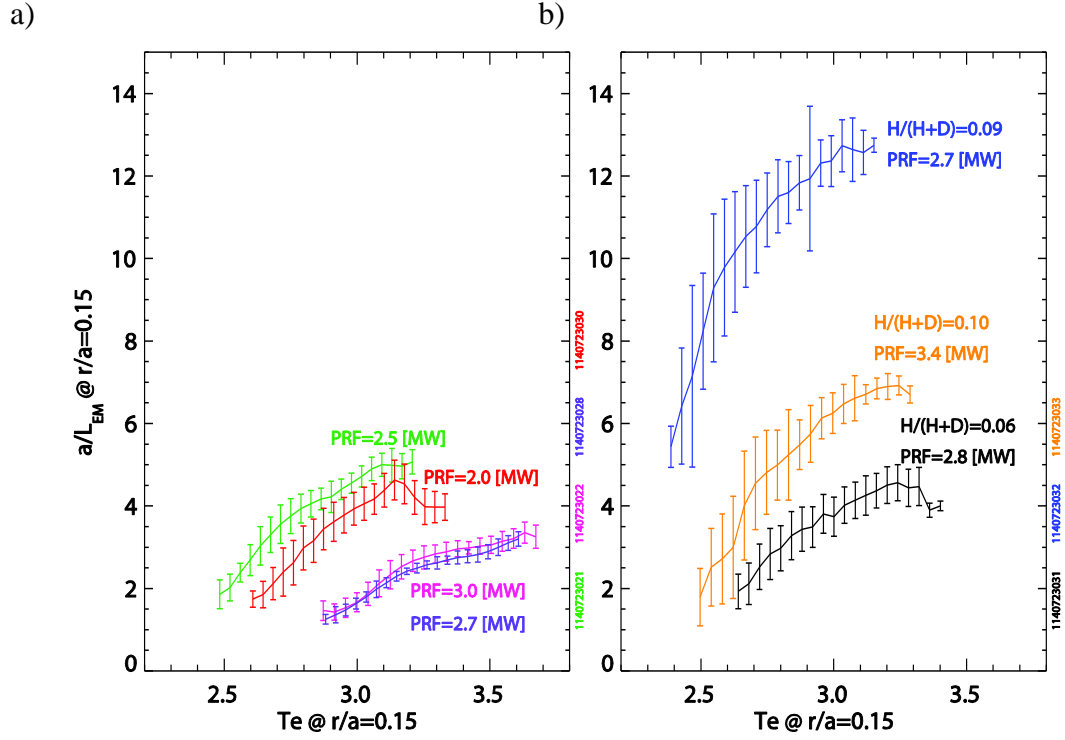


Figure 10. Measured scale length of the soft X-ray radiation at  $\rho = 0.15$  evolving over the sawtooth cycle for a set of 0.52 MA ITER-like Alcator C-Mod H-mode plasmas: (a) ICRF power scan with no extrinsic  $H_2$  puffing indicating a weak change in  $W$  peaking and (b) ICRF and  $H_2$  scan showing a strong change in  $W$  peaking.

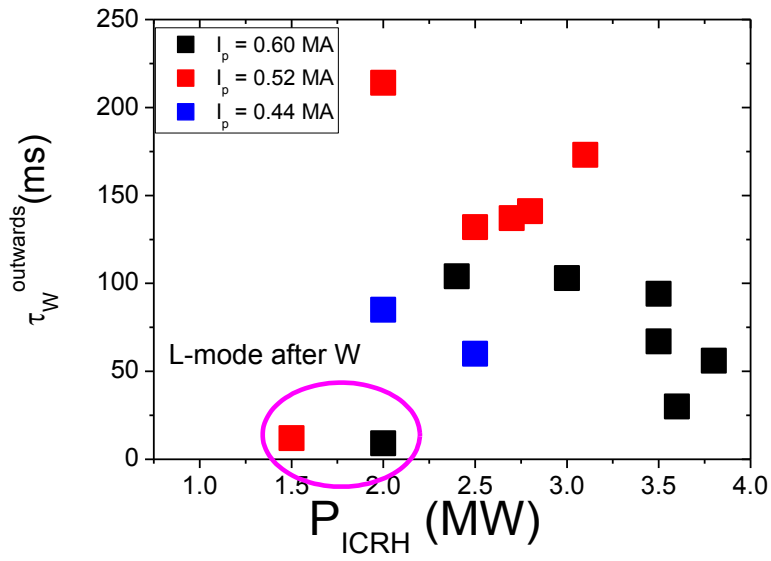


Figure 11. W confinement time versus coupled ICRH power for a set of the Alcator C-Mod ITER-like H-mode discharges. The points highlighted by a magenta circle correspond to discharges in which the W LBO triggers an H-L transition, as shown in Fig. 4.

Case	$q_e^\alpha$ (MWm <sup>-3</sup> )	$q_i^\alpha$ (MWm <sup>-3</sup> )	$q_e^{\text{RF}}$ (MWm <sup>-3</sup> )	$q_i^{\text{RF}}$ (MWm <sup>-3</sup> )
33 MW + 20 MW central ECRH	0.53	0.37	1.0	0
33 MW + 20 MW ICRH with He <sup>3</sup> minority	0.57	0.37	0.6	0.6

Table 1. Power densities deposited in the electron and ions by alpha heating at  $\rho = 0$  for two ITER simulations with  $Q_{\text{DT}} = 10$  and central RF heating (ECRH or ICRH He<sup>3</sup> minority).

Case	$T_e(\rho=0)/T_e(\rho=0.7)$	$T_i(\rho=0)/T_i(\rho=0.7)$	$n_e(\rho=0)/n_e(\rho=0.7)$	$n_i(\rho=0)/n_i(\rho=0.7)$
33 MW + 20 MW central ECRH	3.0	2.7	1.4	1.3
33 MW + 20 MW ICRH with He <sup>3</sup> minority	2.5	2.4	1.5	1.4
Alcator C-Mod $P_{ICRH} = 3.0$ MW	3.3	2.1	1.5	
Alcator C-Mod $P_{ICRH} = 1.5$ MW	3.6	2.8	1.3	

Table 2. Ratios of electron and ion temperatures and electron and ion densities at  $\rho = 0$  and  $\rho = 0.7$  for two ITER simulations with  $Q_{DT} = 10$  and 20 MW of central RF heating (ECRH or ICRH He<sup>3</sup> minority) and two Alcator C-Mod ITER-like H-mode discharges (those of Fig. 5) with two levels of ICRH power heating (1.5 and 3.0 MW).

$T_e (\rho = 0.15)$	$a/L_{ne}$	$a/L_{Te}$	$\frac{T_e}{L_W} \frac{dL_W}{dT_e}$	$a/L_\epsilon$
2.5 keV	0.5	0-1.0	2.5-6.5	3.0-8.0
3.0 keV	0.5	0-1.0	2.2-2.7	2.7-4.2
3.5 keV	0.5	0-1.0	0.6-1.0	1.1-2.5
4.0 keV	0.5	0-1.0	0.0-0.7	0.5-2.2

Table 3. Inverse scale lengths for the electron density, temperature and normalized radiation efficiency at  $\rho = 0.15$  for a range of electron temperatures including their variation along the sawtooth cycle in Alcator C-Mod plasmas. The inverse scale length of the soft X-ray emission ( $a/L_\epsilon$ ) is evaluated from the values in this table and Eq. 5 assuming that  $a/L_{nW} = 0$ .